Exploiting π-π Interactions to Design an Efficient Sorbent for Atrazine Removal from Water

Isil Akpinar,[†,⊥] *Riki J. Drout,*[†,⊥] *Timur Islamoglu,*[†] *Satoshi Kato,*[†] *Jiafei Lyu*[†] *and Omar K. Farha*[*†]

[†]Department of Chemistry, Northwestern University and International Institute of Nanotechnology, 2145 Sheridan Road, Evanston, Illinois 60208, United States

*Corresponding author: o-farha@northwestern.edu

Keywords: Metal–organic frameworks, adsorption, atrazine, adsorption mechanism, π-π interactions

ABSTRACT

The United States Environmental Protection Agency (EPA) recognizes atrazine, a commonly used herbicide, as an endocrine disrupting compound. Excessive use of this agrochemical results in contamination of surface and ground water supplies via agricultural runoff. Efficient removal of atrazine from contaminated water supplies is paramount. Here, the mechanism governing atrazine adsorption in Zr_6-based MOFs has been thoroughly investigated by studying the effects of MOF linker and topology on atrazine uptake capacity and uptake kinetics. We found that the mesopores of NU-1000 facilitated rapid atrazine uptake saturating in < 5 min and that the pyrene-based linkers offered sufficient sites for π-π interactions with atrazine as demonstrated by the near 100% uptake.

Without the presence of a pyrene-based linker, NU-1008, a MOF similar to NU-1000 with respect to surface area and pore size, removed <20% of the exposed atrazine. These results suggest that the atrazine uptake capacity demonstrated by NU-1000 stems from the presence of a pyrene core in the MOF linker, affirming that π-π stacking is responsible for driving atrazine adsorption. Furthermore, NU-1000 displays an exceptional atrazine removal capacity through 3 cycles of adsorption-desorption. Powder X-ray diffraction (PXRD) and Brunauer–Emmett–Teller (BET) surface area analysis confirmed the retention of MOF crystallinity and porosity throughout the adsorption-desorption cycles.

INTRODUCTION

Atrazine, recognized by U.S. Environmental Protection Agency (EPA) as an endocrine disrupting compound and a possible human carcinogen,[1-2] is the second most used herbicide in the United States. Annually, the agricultural industry uses approximately 80 million pounds of atrazine to treat farmland across the nation.[3] Due to its widespread use, persistency, and environmental mobility, atrazine ultimately contaminates surface and ground water supplies. To safeguard aquatic life and human health, the EPA has imposed a maximum contaminant level (MCL) for atrazine in drinking water of 0.003 ppm (3 ppb).[4] Therefore, development of an effective method for removing atrazine from water sources is of utmost importance.

A number of atrazine removal strategies have been reported. Many methods such as coagulation, chlorination, clarification, and filtration are highly inefficient atrazine removal processes.[5-7] Other methods including ozonation,[6] advanced electrochemical,[8] and UV-based[2] oxidation processes display moderate atrazine removal capacity; however, formation of more toxic oxidation by-products and high operational energy costs limit the widespread implementation of these techniques. Alternatively, adsorption is an effective, relatively less expensive, and harmless method, that demonstrates promise in resolving atrazine contamination.[9-10] Specifically, activated carbon,[11] zeolites,[12] resins,[13] clay materials,[14] and biochar[15] have been examined as sorbents for atrazine removal. Unfortunately, though widely used, activated carbon is a moderately expensive strategy for water treatment because the low volumetric capacities necessitate the use of excessive amounts of sorbent.[16-17] Regeneration of porous carbons also remains challenging.[18] Further, carbon-based materials, including carbon nanotubes and porous carbons, often require long exposure times to reach saturation capacity.[19-20] Therefore, a recyclable, high capacity material to remove organic contaminants from water must be designed to ensure cost efficiency. We anticipate that the hierarchical porous structure and dense chemical functionality characteristic of metal–organic frameworks (MOFs) will afford both rapid uptake kinetics and high uptake capacity, respectively.

The properties displayed by MOFs, namely porosity and crystallinity, make them potential candidates for atrazine sorption. MOFs are comprised of inorganic nodes and organic linkers that assemble into multidimensional periodic lattices through coordination bonds.[21-22] Through judicious choice of node and linker and/or *via* a host of post-synthetic modification techniques, these crystalline materials can be chemically and structurally tuned to yield various pore sizes and shapes, surface areas, and chemical functionality.[23-25] Because of their tailorable properties, MOFs have been utilized for numerous applications including, but not limited to, gas storage and separation,[26-30] catalysis,[31-36] drug delivery,[37-38] chemical separation,[39-40] detoxification of chemical warfare agents,[41-42] and water remediation.[43-45]

Importantly, Zr_6-based MOFs demonstrate exceptional water stability owing to their strong Zr(IV)–O bonds.[23, 46] Therefore, such materials have been investigated for the capture of arsenic, rhenium, and selenium oxyanions.[43, 47-48] Given MOF crystallinity, single-crystal X-ray diffraction can be utilized to elucidate the binding motif; for example, perrhenate binds at the Zr_6-node of NU-1000 through displacement of the terminal water ($–OH_2$) and hydroxyl (–OH) groups. Further, MOF linkers can also serve as potential adsorption sites. For example, sorption of aldehyde- over carboxylic acid-functionalized phenolics in NU-1000 has been attributed to π-π interactions between the analyte and the pyrene-based linker.[49] Herein, we capitalize on the precise synthetic designability of MOFs to systematically tune MOF structure and chemical functionality to investigate the mechanism driving atrazine adsorption from water.

To this end, we chose to investigate atrazine sorption in Zr_6-based MOFs with a variety of pore sizes and linker functionalities. We hypothesized that π-π interactions govern atrazine sorption and therefore investigated a series of MOFs comprised of linkers with increasingly large conjugated π-systems (Figure 1). Considering the assortment of linkers, NU-1000 and NU-901, both of which contain the pyrene-based linker, H_4TBAPy, were expected to display the highest atrazine uptakes. While consisting of the same node and linker, the larger pores of NU-1000 compared to NU-901 were predicted to facilitate diffusion and afford faster atrazine uptake. Though similar to NU-1000 with respect to surface area and pore size, NU-1008 does not contain a pyrene-based linker and is expected to exhibit a lower atrazine affinity. Following a preliminary screening, NU-1000 was fully analyzed to determine its maximum atrazine uptake capacity, selectivity in the presence of salt, recyclability, and stability to the adsorption-desorption process.

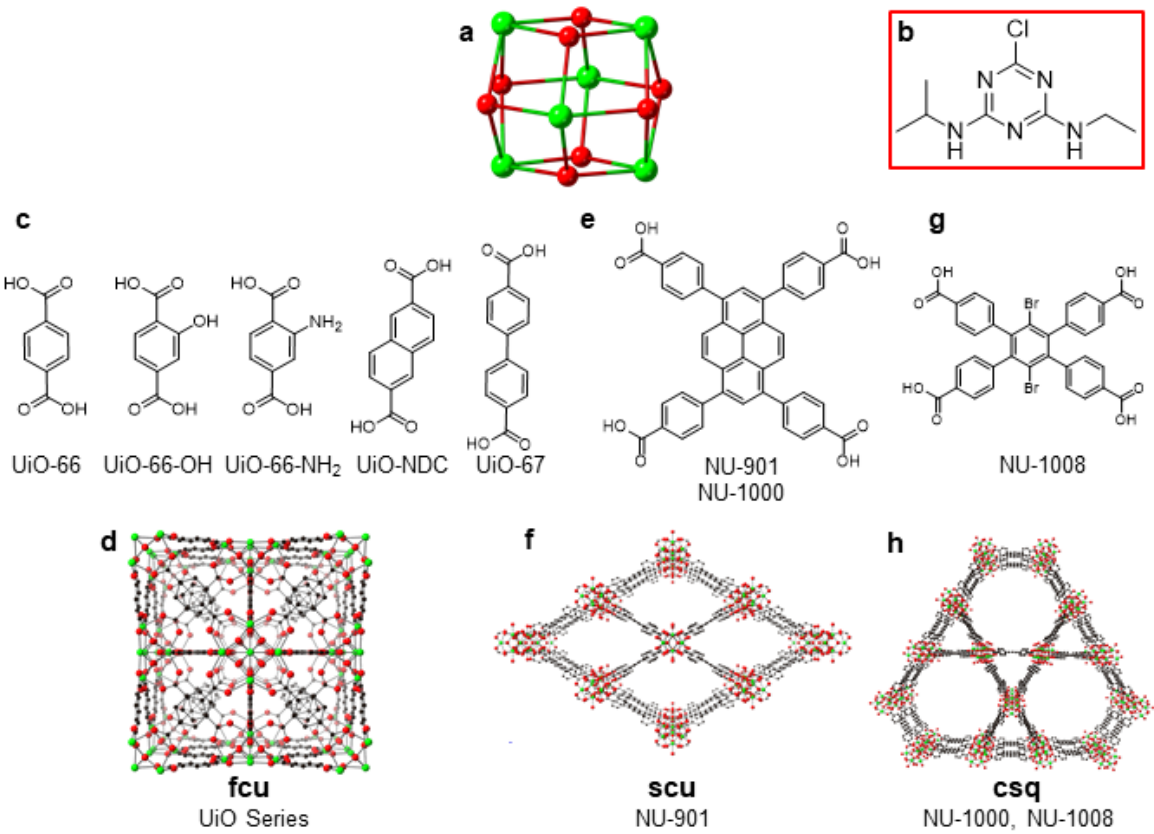

Figure 1. The structures of a) the Zr_6-node, b) atrazine, c) linkers for UiO-66, UiO-66-OH, UiO-66-NH_2, UiO-NDC and UiO-67, d) UiO series topology, e) linker for NU-1000 and NU-901 and f) NU-901 topology, g) linker for NU-1008, and h) NU-1000 and NU-1008 topology.

EXPERIMENTAL DETAILS

Chemicals: All chemicals were purchased from commercial suppliers and used as received. Specifically, atrazine was purchased from Sigma-Aldrich. Water in all experiments is Milli-Q (milli-pore). In all HPLC-diode array detector (DAD) experiments, HPLC-grade acetone was used. All gases were Ultra High Purity grade 5 gases from Airgas Specialty Gases.

General Experimental: UiO-66, UiO-66-OH, UiO-66-NH_2, UiO-67, UiO-NDC, NU-901, NU-1008 and NU-1000 were prepared according to reported protocols.[50-52] Detailed syntheses are provided in the Supporting Information for convenience. All MOF samples were thermally activated under ultrahigh vacuum at 120 ºC for 12 h on a Micromeritics Smart VacPrep. Nitrogen adsorption and desorption isotherm measurements were collected at 77 K on a Micromeritics Tristar II. Powder X-ray diffraction measurements were obtained using a STOE STADI MP equipped with a Kα1 source and a 1D strip detector over a range of $2^\circ \leq 2\theta \leq 30^\circ$. Scanning electron microscopy (SEM) samples were prepared by drop casting and coated with a ~9 nm thick layer of OsO_4 using a Denton Desk III TSC Sputter Coater. SEM images were collected on a Hitachi SU8030. HPLC experiments were performed on an HPLC Agilent 1100 series system coupled with a diode-array detector (DAD). The reverse phase HPLC column, C18 (Supelco, Ascentis® C18, 150 mm x 4.6 mm, 5 μm particle) was used with a water/acetonitrile mobile phase (50:50 v/v) at a flow rate of 1 mL min^{-1}. The detector was set to a wavelength of 223 nm and the column temperature was set to 25°C. HPLC standards were prepared via serial dilution in water. All experiments were performed in triplicate.

Screening of Atrazine Affinity: Initial experiments were performed to evaluate the atrazine affinity of Zr_6-based MOFs, namely, UiO-66 UiO-66-OH, UiO-66-NH_2, UiO-67, UiO-67-NDC, NU-1008, NU-901 and NU-1000. In a typical experiment, an activated MOF sample (3.5 mg) was exposed to 10 mL of a 10 ppm aqueous atrazine solution in a 4-dram glass vial. The vials were agitated at ambient temperature for 24 h to ensure constant mixing and to allow sufficient time to reach saturation uptake. After 24 h, an aliquot (1 mL) of the solution was removed using a disposable syringe equipped with a 0.45 μm PDVF syringe filter. The atrazine concentration was quantified by HPLC-DAD. The amount of atrazine adsorbed by the MOF was determined by comparing these concentrations to the concentration of a 10 ppm atrazine solution without MOF. Percent adsorption uptake was calculated using eq 1:

$$\mathrm{Uptake}\ (\%) = \frac{C_i - C_e}{C_i} \times 100 \qquad \text{(Eq. 1)}$$

where C_i and C_e (mg L^{-1}) are the initial and equilibrium concentrations, respectively.

Kinetic Screening Studies: To investigate the kinetics of atrazine adsorption, samples of NU-1000 (3.5 mg) were exposed to 10 mL of an aqueous 10 ppm atrazine solution in 4-dram glass vials. After a designated time (1, 5, 30, 60 and 120 min), 1 mL aliquots were removed with a disposable syringe equipped with a 0.45 μm PDVF syringe filter. The initial and equilibrium atrazine concentrations in each solution were determined as previously described via HPLC-DAD. The amount of atrazine uptake q in mg of atrazine per gram of MOF was determined at each time point according to eq 2:

$$q = \frac{(C_i - C_f)\,V}{m} \qquad \text{(Eq. 2.)}$$

where C_i is the initial concentration (mg L^{-1}), C_f is the final concentration (mg L^{-1}), V is the volume of solution exposed to sorbent (L), and m is the mass of sorbent (g).

Maximum Adsorption Capacity of NU-1000: To determine the maximum atrazine adsorption capacity of NU-1000, MOF samples (3.5 mg) were exposed to 10 mL of aqueous atrazine solutions with atrazine concentrations of 1, 2, 4, 6, or 8 ppm in 4-dram glass vials. After 2 h, aliquots of the supernatant were removed using a disposable syringe equipped with a 0.45 μm PDVF syringe filter and analyzed by HPLC-DAD. The amount of atrazine adsorbed by the MOF was determined again by comparing these concentrations to the concentration of control solutions without MOF.

Effect of Ionic Strength on Adsorption: To investigate the effect of ionic strength on atrazine adsorption, NU-1000 samples (3.5 mg) were exposed to 10 mL of a 10 ppm aqueous atrazine solution in 0.1 M sodium chloride, 0.1 M sodium nitrate, 0.1 M sodium sulfate, or 0.1 M calcium chloride. After 1 h, an aliquot (1 mL) was removed with a disposable syringe equipped with a 0.45 μm PDVF syringe filter. The initial and equilibrium atrazine concentrations were determined by HPLC-DAD.

Regeneration of NU-1000: The regeneration of NU-1000 was explored first by exposing a MOF sample (10 mg) to 10 mL of an aqueous 10 ppm atrazine solution in a 4-dram glass vial. The mixture was agitated at ambient temperature for 24 h. The slurry was then centrifuged to allow the MOF to settle and the supernatant was decanted. The atrazine-saturated NU-1000 sample was then soaked in 1 mL of acetone and agitated for 12 h. Similarly, this sample was centrifuged to settle the MOF and the supernatant was decanted. NU-1000 was then soaked again in 1 mL of acetone for 12 h and then centrifuged to settle the MOF and the supernatant was decanted. Finally, NU-1000 was dried in a vacuum oven at 80 ºC for 12 h. This adsorption-desorption cycle was performed a total of three cycles.

RESULTS AND DISCUSSION

Screening of Atrazine Affinity: Preliminary studies were performed to investigate the atrazine affinity of several Zr_6-based MOFs (Table 1 and Figure 2). UiO-66, and its derivatives, UiO-67, and UiO-NDC are composed of 12-connected Zr_6-nodes and dicarboxylate organic linkers (Figure 1a). The linkers in UiO-66, UiO-66-OH, and UiO-66-NH_2 are 1,4-benzenedicarboxylate (BDC), 2-hydroxy-1,4 benzenedicarboxylate (BDC-OH), and 2-amino-1,4 benzenedicarboxylate (BDC-NH_2), respectively. These derivatives of UiO-66 were synthesized to evaluate the effect of linker functional groups on atrazine uptake. Additionally, UiO-67 and UiO-NDC, which feature the extended linkers biphenyl-4,4′-dicarboxylate (BPDC) and 2,6 napthalenedicarboxylate (NDC), respectively, were chosen because their linkers contain larger π-systems compared to the UiO-66 series which may contribute to greater atrazine uptake. To further investigate the role of π-π interactions in the adsorption process, NU-1000 and NU-901 which consist of Zr_6-nodes and the pyrene-based linker, 1,3,6,8-tetrakis(p-benzoic acid)pyrene (H_4TBAPy), were examined (Figure 1b). The framework of NU-1000 is characterized by 12 Å triangular and 31 Å hexagonal 1D channels connected by small windows (~8 Å);[53] whereas NU-901 displays diamond-shaped 1D channels with an aperture of 12 Å.

In a traditional screening experiment, an activated MOF sample was exposed to an aqueous atrazine solution. UiO-66 and UiO-66-NH_2 were found to adsorb a mere 2% of the total atrazine in solution, and UiO-66-OH adsorbed only 3%. Such low uptake amounts suggest that atrazine is unable to diffuse into the small pores of UiO-66 and its derivates and could only adsorb to the particle surface. Additionally, the hydrogen bonding potential of the functional groups did not increase the atrazine adsorption capacity likely because atrazine cannot displace the water molecules hydrogen bonding to the functional groups on the linkers (i.e. –NH_2, –OH) while the MOFs are submersed in water. The extended linker of UiO-67 increases the pore size facilitating diffusion and offers more atrazine adsorption sites as demonstrated by a moderate atrazine removal efficiency of 40%. While the pores of UiO-NDC are slightly smaller than those of UiO-67, the MOF displays a higher atrazine removal capacity (54%) presumably due to the increased π-π interaction potential of the naphthalene linker.

Upon incorporation of a pyrene-based linker, the atrazine removal capacity dramatically increased. NU-901, while it has smaller pores than both UiO-67 and UiO-NDC, removed 84% of the atrazine in the solution to which it was exposed. This high atrazine removal efficiency can be attributed to the pyrene core of the H_4TBAPy linker which enhances the removal capacity through the increased availability of π-π interactions. Of all MOFs investigated, NU-1000 demonstrated the most efficient atrazine adsorption behavior removing 95% of the atrazine in solution. In comparison to the pores of NU-901, the hexagonal pores of NU-1000 are larger further enhancing diffusion and increasing the atrazine capacity per pore. To confirm pore size was not the primary factor contributing to the enhanced atrazine uptake in NU-901 and NU-1000 compared to the UiO

MOFs, NU-1008 was examined. NU-1008 has similar pore size and surface area to NU-1000; however, its linker does not contain a pyrene moiety. The low atrazine removal capacity of NU-1008 (13%) reinforces that π-π interactions between atrazine and the pyrene-based linker present in NU-1000 and NU-901 are the primary interactions driving atrazine adsorption.

Table 1. The surface areas, pore sizes, and approximate pore apertures of Zr_6-based MOFs screened for atrazine adsorption. [a] Reported pore aperture sizes of UiO series MOFs are measured for the node-to-node distance of the tetrahedral pore.[54]

MOF	Surface Area (m^2 g^{-1})	Pore Size (Å)	Pore Aperture (Å)[a]
UiO-66	1690	12 and 16	7.5
UiO-66-NH_2	1410	13	7.5
UiO-66-OH	1210	11	7.5
UiO-67	2510	13 and 23	12
UiO-NDC	1960	12 and 20	9
NU-1008	1400	14 and 30	14 and 30
NU-901	2110	12	12
NU-1000	2210	12 and 30	12 and 30

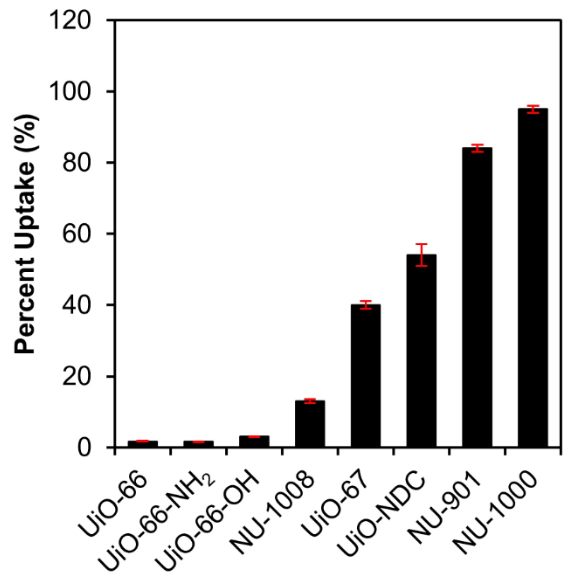

Figure 2. Atrazine adsorption uptake as a percentage of the total amount of atrazine exposed to MOF samples (3.5 mg of MOF exposed to 10 mL of 10 ppm atrazine solution under ambient conditions for 24h).

Kinetic Studies: Rapid uptake of the target contaminant is critical in evaluating the feasibility of water purification methods given that large amounts of liquid must be treated efficiently. To this end, the kinetics of atrazine adsorption in UiO-NDC, NU-1008, NU-901 and NU-1000 were investigated. Specifically, MOF samples were exposed to identical 10 ppm atrazine solutions and the concentration of atrazine in solution was analyzed at several time points (Figure 3). Within 1 min, NU-1000 captures 93% of the atrazine in the test solution equivalent to 98% of its saturation uptake. The rapid atrazine uptake kinetics are most likely attributed to the periodicity of the MOF lattice, the large pores of NU-1000 that facilitate diffusion, and the easily accessible and highly abundant pyrene-based linkers. NU-901 displays slightly slower kinetics than NU-1000, reaching 85% of its saturation uptake within 1 min to capture 75% of the exposed atrazine. While NU-901 displays rather efficient uptake, the slower saturation is believed to stem from the framework's smaller pores in comparison to NU-1000. Similarly, within 1 min, UiO-NDC removes 44% of the exposed atrazine, and while this is a relatively low uptake amount, it is equivalent to 82% of the atrazine saturation capacity of UiO-NDC. Of the MOFs investigated, NU-1008 exhibits the slowest kinetics capturing only 69% after its saturation capacity within 1 min equivalent to a mere 9% of the exposed atrazine. If pore size was the main contributing factor, the kinetics of atrazine uptake in NU-1008 should exceed those of both UiO-NDC and NU-901; however, this is not the case. Comparing NU-1000 and NU-901 suggests that pore size contributes slightly to rapid uptake saturation; however, the availability of π-π interactions present in NU-1000, NU-901, and UiO-NDC are primarily responsible for driving rapid atrazine uptake given the pore sizes vary dramatically between the three MOFs. These results suggest that pore size and the availability of π-π interactions at adsorption sites concomitantly influence atrazine capture kinetics.

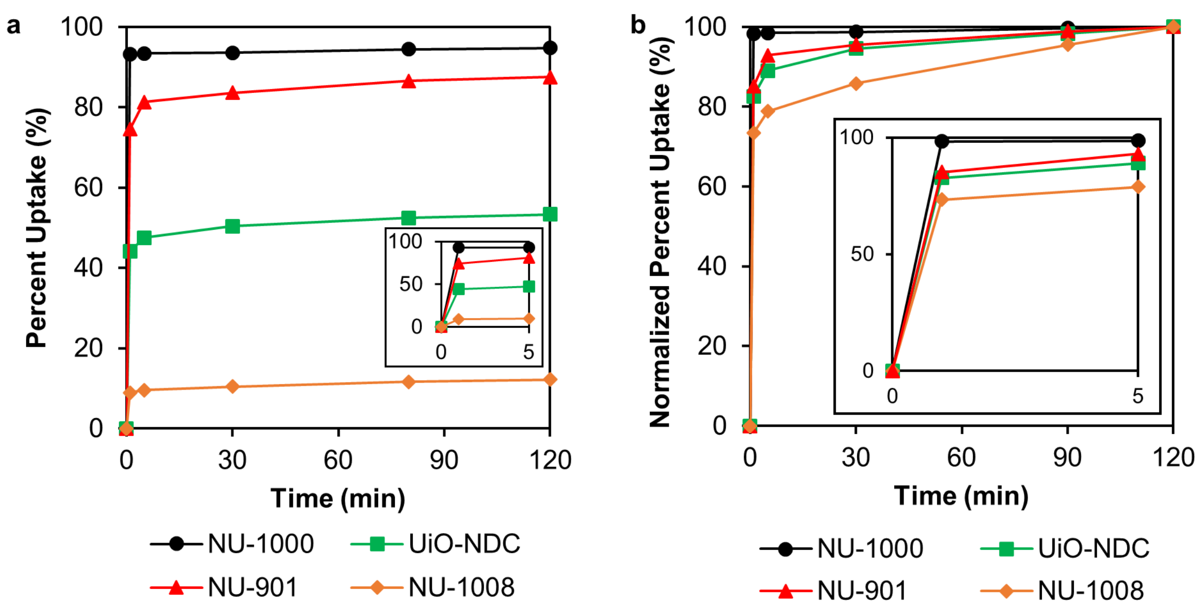

Figure 3. a) Atrazine adsorption isotherms as percent (%) uptake of atrazine exposed versus time for various MOFs. b) Atrazine adsorption isotherms as normalized percent (%) of respective saturation uptake versus time for various MOFs. Insets show the uptake between 0 and 5 min.

Adsorption Capacity of NU-1000: The exceptional and rapid atrazine adsorption demonstrated by NU-1000 prompted us to determine its maximum atrazine uptake capacity. To do so, MOF samples were exposed to aqueous solutions with various atrazine concentrations. Adsorption isotherms were constructed for each exposure concentration by determining the amount q of atrazine (mg) adsorbed by the MOF (g) at various time points using eq 1. The equilibrium atrazine concentration in solution was determined by HPLC-DAD and used to calculate the amount of atrazine adsorbed at equilibrium. A Type-I Langmuir fit (Figure S5) revealed a maximum atrazine uptake capacity of 36 mg of atrazine per gram of NU-1000 (Figure S5, Table S1, and Table S2).[20, 55-61] The associated Langmuir constant (K_L) value of 1.78 L mg^{-1} low time to saturation for atrazine adsorption in NU-1000 indicates that NU-1000 displays a greater affinity for atrazine and more favorable sorption kinetics than most materials reported for atrazine adsorption (Table 2).

Table 2. Comparison of Langmuir constant values reported for atrazine adsorption on various materials reveals that NU-1000 outperforms most reported materials with respect to uptake capacity and sorption kinetics.

Adsorbents	K_L Langmuir Constant (L mg^{-1})	Time to Saturation	Reference
NU-1000	1.78	< 1 min	This work
Carbon nanotube – r-MWNT	1.47 (at 25°C)	6 h	56
Carbon nanotube - SMWNT20	0.96 (at 25°C)	6 h	56
Multiwalled carbon nanotubes	0.7710	7 h	20
Biochar - CS450	0.618 (at 25°C)	N/A	57
Polyacrylic acid-functionalized magnetic ordered mesoporous carbon (P-MMC)	0.2058	24 h	59
Biochar - ADPCS450	0.196 (at 25°C)	N/A	57
Treated banana peels	0.12 (at 25°C)	15 h	60
Ordered mesoporous carbon (OMC)	0.1130	24 h	59
Magnetic ordered mesoporous carbon (MMC)	0.1089	24 h	59

Sludge-based activated carbon-like material	0.05	10 h	[61]

Effect of Ionic Strength on Adsorption: Equally important as rapid saturation and high uptake capacity is selectivity for the target contaminant even in the presence of competing interferents. Given their abundance in water sources, sodium chloride, sodium nitrate, sodium sulfate, and calcium chloride were used to investigate the selectivity of NU-1000 for atrazine in the presence of competing ions (Figure 4). As such, MOF samples were exposed to a 10 ppm aqueous atrazine solution or a 10 ppm aqueous atrazine solution in 0.1 M NaCl, $NaNO_3$, Na_2SO_4, or $CaCl_2$. NU-1000 was found to remove 94% of the atrazine from pure water and 93%, 92%, 97%, and 97% of the total exposed atrazine from the 0.1 M NaCl, 0.1 M $NaNO_3$, 0.1 M Na_2SO_4, and 0.1 M $CaCl_2$ solutions, respectively. Therefore, the presence of competing salts does not significantly affect the atrazine affinity of NU-1000 suggesting NU-1000 may be a promising material for adsorptive atrazine removal.

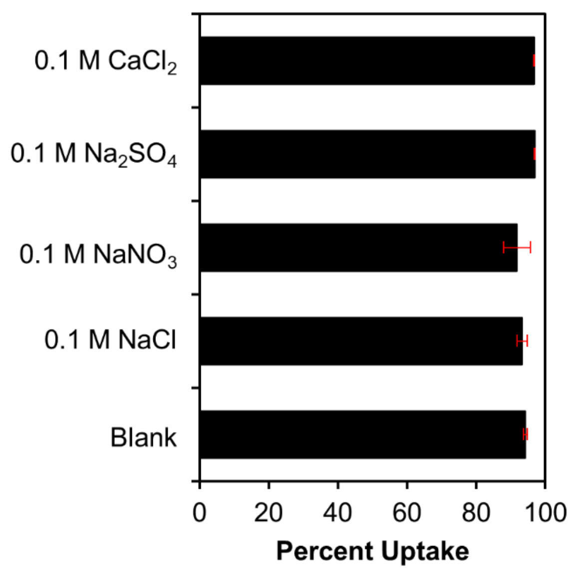

Figure 4. NU-1000 maintains its atrazine affinity in the presence of competing salt ions.

Regeneration and Stability of NU-1000: A sorbent's cost efficiency can be significantly enhanced if the material can be regenerated after adsorption and reused for many additional adsorption-desorption cycles. Atrazine is highly soluble in acetone (31 g L^{-1} at 25 ˚C); therefore, this solvent was chosen to study the recyclability of NU-1000.[62] In a typical experiment, a MOF sample was loaded with atrazine and then treated with acetone at room temperature. Through three cycles of the adsorption-desorption process, NU-1000 efficiently removed atrazine without significant decrease in efficiency (Figure 5a). Moreover, through this process, the structural integrity and porosity of NU-1000 are retained as demonstrated by powder X-ray diffraction patterns (PXRD) (Figure 5b) and N_2 adsorption-desorption isotherms (Figure S8), respectively.

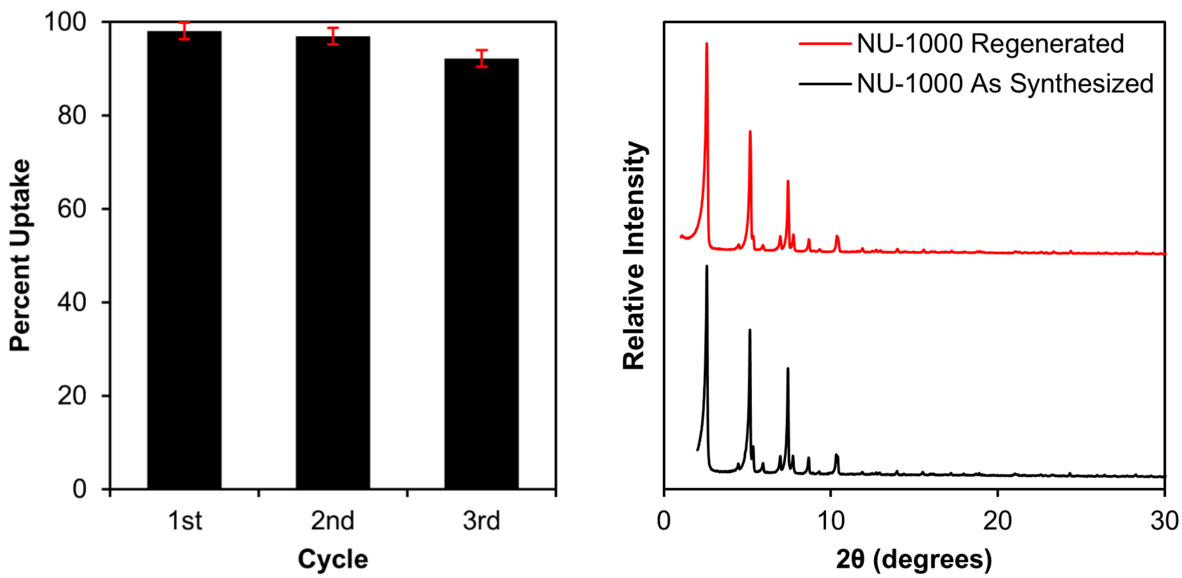

Figure 5. Through three cycles of atrazine adsorption and regeneration with acetone, a) NU-1000 shows only a slight decrease in atrazine uptake and b) retains its bulk structural integrity as demonstrated by PXRD.

CONCLUSION

In summary, we capitalized on the synthetic tunability of MOFs to systematically investigate the role of chemical functionality, specifically π-system size, in the adsorptive removal of atrazine from water. In preliminary screenings, the atrazine affinity of a selection of Zr-based MOFs with various linker π-system sizes and chemical functionality, framework topologies, and pore sizes was assessed. NU-1000, NU-901, and UiO-NDC displayed the highest atrazine affinities suggesting that π-π interactions are the primary contributor to atrazine adsorption. A thorough investigation of atrazine uptake kinetics in UiO-NDC, NU-901, NU-1008, and NU-1000 further corroborated that the presence of linkers with extended π-systems, rather than large pores results in the exceptional atrazine uptake demonstrated by NU-1000. Additionally, NU-1000 was found to reach its maximum capacity within 1 min likely due to the framework's large pores which facilitate diffusion and the abundance of potential π-π interaction sites at the pyrene-based linkers. NU-1000 was fully evaluated for atrazine adsorption and found to have a maximum adsorption capacity of 36 mg of atrazine per g of NU-1000. Although this capacity is comparable to that of other sorbents that have been used for atrazine adsorption, 98% of its saturation atrazine uptake is attained within 1 min, again because of rapid diffusion through the hierarchically porous MOF structure. Moreover, in the presence of competing salt ions, NU-1000 maintains its atrazine affinity. Furthermore, after atrazine adsorption, NU-1000 can be easily regenerated by acetone washing while retaining at least 99% of its original atrazine uptake. Given that its large pores and pyrene-based linkers facilitate rapid and exceptionally high atrazine uptake, NU-1000 is a promising candidate for adsorptive atrazine removal.

ASSOCIATED CONTENT

Supporting Information

Nitrogen adsorption isotherms, pore size distributions, PXRD patterns, adsorption capacity data, and SEM images. This information is available free of charge on the ACS Publications website at DOI: X.

AUTHOR INFORMATION

Corresponding Author

*E-mail: o-farha@northwestern.edu.

Notes

⊥These authors contributed equally.

The authors declare no competing financial interest.

ACKNOWLEDGMENT

O.K.F. gratefully acknowledges the support of the Nanoporous Materials Genome Center, funded by the U.S. DOE, Office of Science, Basic Energy Sciences Program (Award DE-FG02-17ER16362). R.J.D. appreciates the support of the Northwestern University Ryan Fellowship granted by the International Institute of Nanotechnology and The Graduate School. This work made use of the EPIC, Keck-II, and SPID facilities of Northwestern University's NUANCE Center, which has received support from the Soft and Hybrid Nanotechnology Experimental (SHyNE) Resource (NSF ECCS-1542205); the MRSEC program (NSF DMR-1121262) at the Materials Research Science and Engineering Center; the International Institute for Nanotechnology (IIN); the Keck Foundation; and the State of Illinois, through the IIN.

REFERENCES

1. Environmental Protection Agency, U. S. Edsp: Weight of Evidence Analysis of Potential Interaction with the Estrogen, Androgen or Thyroid Pathyways. https://www.epa.gov/endocrine-disruption/endocrine-disruptor-screening-program-tier-1-screening-determinations-and (accessed 1 June 2018).
2. Kong, X.; Jiang, J.; Ma, J.; Yang, Y.; Liu, W.; Liu, Y., Degradation of Atrazine by Uv/Chlorine: Efficiency, Influencing Factors, and Products. *Water Res.* **2016,** *90*, 15-23.
3. Runes, H. B.; Bottomley, P. J.; Lerch, R. N.; Jenkins, J. J., Atrazine Remediation in Wetland Microcosms. *Environ. Toxicol. Chem.* **2001,** *20* (5), 1059-1066.
4. United States Environmental Protection Agency National Primary Drinking Water Regulations. https://www.epa.gov/ground-water-and-drinking-water/national-primary-drinking-water-regulations (accessed 16 June 2018).
5. Brown, N. W.; Roberts, E. P. L.; Chasiotis, A.; Cherdron, T.; Sanghrajka, N., Atrazine Removal Using Adsorption and Electrochemical Regeneration. *Water Res.* **2004,** *38* (13), 3067-3074.
6. Broseus, R.; Vincent, S.; Aboulfadl, K.; Daneshvar, A.; Sauve, S.; Barbeau, B.; Prevost, M., Ozone Oxidation of Pharmaceuticals, Endocrine Disruptors and Pesticides During Drinking Water Treatment. *Water Res.* **2009,** *43* (18), 4707-4717.
7. Gomes, J.; Costa, R.; Quinta-Ferreira, R. M.; Martins, R. C., Application of Ozonation for Pharmaceuticals and Personal Care Products Removal from Water. *Sci. Total Environ.* **2017,** *586*, 265-283.
8. Komtchou, S.; Dirany, A.; Drogui, P.; Robert, D.; Lafrance, P., Removal of Atrazine and Its by-Products from Water Using Electrochemical Advanced Oxidation Processes. *Water Res.* **2017,** *125*, 91-103.
9. Ali, I.; Gupta, V. K., Advances in Water Treatment by Adsorption Technology. *Nat. Protoc* **2007,** *1*, 2661-2667.
10. Ali, I., Water Treatment by Adsorption Columns: Evaluation at Ground Level. *Sep. Purif. Rev.* **2014,** *43* (3), 175-205.
11. Chingombe, P.; Saha, B.; Wakeman, R. J., Sorption of Atrazine on Conventional and Surface Modified Activated Carbons. *J. Colloid Interface Sci.* **2006,** *302* (2), 408-416.
12. Lemic, J.; Kovacevic, D.; Tomasevic-Canovic, M.; Kovacevic, D.; Stanic, T.; Pfend, R., Removal of Atrazine, Lindane and Diazinone from Water by Organo-Zeolites. *Water Res.* **2006,** *40* (5), 1079-1085.
13. Doulia, D.; Hourdakis, A.; Rigas, F.; Anagnostopoulos, E., Removal of Atrazine from Water by Use of Nonionic Polymeric Resins. *J. Environ. Sci. Health A* **2008,** *32* (9-10), 2635-2656.
14. Sanchez-Martin, M. J.; Rodriguez-Cruz, M. S.; Andrades, M. S.; Sanchez-Camazano, M., Efficiency of Different Clay Minerals Modified with a Cationic Surfactant in the Adsorption of Pesticides: Influence of Clay Type and Pesticide Hydrophobicity. *Appl. Clay Sci.* **2006,** *31* (3-4), 216-228.
15. Tan, G.; Sun, W.; Xu, Y.; Wang, H.; Xu, N., Sorption of Mercury (Ii) and Atrazine by Biochar, Modified Biochars and Biochar Based Activated Carbon in Aqueous Solution. *Bioresour. Technol.* **2016,** *211*, 727-735.
16. Mohan, D.; Pittman, C. U., Arsenic Removal from Water/Wastewater Using Adsorbents—a Critical Review. *J. Hazard. Mater.* **2007,** *142* (1), 1-53.

17. Xu, J.; Wang, L.; Zhu, Y., Decontamination of Bisphenol a from Aqueous Solution by Graphene Adsorption. *Langmuir* **2012,** *28* (22), 8418-8425.
18. Gupta, V. K.; Saleh, T. A., Sorption of Pollutants by Porous Carbon, Carbon Nanotubes and Fullerene- an Overview. *Environ. Sci. Pollut. Res.* **2013,** *20* (5), 2828-2843.
19. Zhang, W.; Zheng, J.; Zheng, P.; Qiu, R., Atrazine Immobilization on Sludge Derived Biochar and the Interactive Influence of Coexisting Pb(Ii) or Cr(Vi) Ions. *Chemosphere* **2015,** *134*, 438-445.
20. Tang, W.-W.; Zeng, G.-M.; Gong, J.-L.; Liu, Y.; Wang, X.-Y.; Liu, Y.-Y.; Liu, Z.-F.; Chen, L.; Zhang, X.-R.; Tu, D.-Z., Simultaneous Adsorption of Atrazine and Cu (Ii) from Wastewater by Magnetic Multi-Walled Carbon Nanotube. *Chem. Eng. J.* **2012,** *211-212*, 470-478.
21. Hailian Li, M. E., M. O`Keeffe & O.M. Yaghi, Design and Synthesis of an Exceptionally Stable and Highly Porous Metal-Organic Framework. *Nature* **1999,** *402*, 276-279.
22. Furukawa, H.; Cordova, K. E.; O'Keeffe, M.; Yaghi, O. M., The Chemistry and Applications of Metal-Organic Frameworks. *Science* **2013,** *341*, 1230444.
23. Howarth, A. J.; Liu, Y.; Li, P.; Li, Z.; Wang, T. C.; Hupp, J. T.; Farha, O. K., Chemical, Thermal and Mechanical Stabilities of Metal–Organic Frameworks. *Nat Rev Mater.* **2016,** *1* (3), 1-15.
24. Susumu, K.; Ryo, K.; Shin-ichiro, N., Functional Porous Coordination Polymers. *Angew. Chem. Int. Ed.* **2004,** *43* (18), 2334-2375.
25. Wang, Z.; Cohen, S. M., Postsynthetic Modification of Metal–Organic Frameworks. *Chem. Soc. Rev.* **2009,** *38* (5), 1315-1329.
26. Rosi, N. L.; Eckert, J.; Eddaoudi, M.; Vodak, D. T.; Kim, J.; O'Keeffe, M.; Yaghi, O. M., Hydrogen Storage in Microporous Metal-Organic Frameworks. *Science* **2003,** *300* (5622), 1127-1129.
27. Li, J. R.; Kuppler, R. J.; Zhou, H. C., Selective Gas Adsorption and Separation in Metal-Organic Frameworks. *Chem. Soc. Rev.* **2009,** *38* (5), 1477-504.
28. Nugent, P.; Belmabkhout, Y.; Burd, S. D.; Cairns, A. J.; Luebke, R.; Forrest, K.; Pham, T.; Ma, S.; Space, B.; Wojtas, L.; Eddaoudi, M.; Zaworotko, M. J., Porous Materials with Optimal Adsorption Thermodynamics and Kinetics for Co2 Separation. *Nature* **2013,** *495*, 80-84.
29. Xue, D.-X.; Cairns, A. J.; Belmabkhout, Y.; Wojtas, L.; Liu, Y.; Alkordi, M. H.; Eddaoudi, M., Tunable Rare-Earth Fcu-Mofs: A Platform for Systematic Enhancement of Co2 Adsorption Energetics and Uptake. *J. Am. Chem. Soc.* **2013,** *135* (20), 7660-7667.
30. Alezi, D.; Belmabkhout, Y.; Suyetin, M.; Bhatt, P. M.; Weseliński, Ł. J.; Solovyeva, V.; Adil, K.; Spanopoulos, I.; Trikalitis, P. N.; Emwas, A.-H.; Eddaoudi, M., Mof Crystal Chemistry Paving the Way to Gas Storage Needs: Aluminum-Based Soc-Mof for Ch4, O2, and Co2 Storage. *J. Am. Chem. Soc.* **2015,** *137* (41), 13308-13318.
31. Schlichte, K.; Kratzke, T.; Kaskel, S., Improved Synthesis, Thermal Stability and Catalytic Properties of the Metal-Organic Framework Compound Cu3(Btc)2. *Microporous Mesoporous Mater.* **2004,** *73* (1), 81-88.
32. Lee, J.; Farha, O. K.; Roberts, J.; Scheidt, K. A.; Nguyen, S. T.; Hupp, J. T., Metal-Organic Framework Materials as Catalysts. *Chem. Soc. Rev.* **2009,** *38* (5), 1450-1459.
33. Bai, Y.; Dou, Y.; Xie, L. H.; Rutledge, W.; Li, J. R.; Zhou, H. C., Zr-Based Metal-Organic Frameworks: Design, Synthesis, Structure, and Applications. *Chem. Soc. Rev.* **2016,** *45* (8), 2327-2367.

34. Comito, R. J.; Fritzsching, K. J.; Sundell, B. J.; Schmidt-Rohr, K.; Dincă, M., Single-Site Heterogeneous Catalysts for Olefin Polymerization Enabled by Cation Exchange in a Metal-Organic Framework. *J. Am. Chem. Soc.* **2016,** *138* (32), 10232-10237.
35. Grigoropoulos, A.; Whitehead, G. F. S.; Perret, N.; Katsoulidis, A. P.; Chadwick, F. M.; Davies, R. P.; Haynes, A.; Brammer, L.; Weller, A. S.; Xiao, J.; Rosseinsky, M. J., Encapsulation of an Organometallic Cationic Catalyst by Direct Exchange into an Anionic Mof. *Chem. Sci.* **2016,** *7* (3), 2037-2050.
36. Islamoglu, T.; Ortuno, M. A.; Proussaloglou, E.; Howarth, A. J.; Vermeulen, N. A.; Atilgan, A.; Asiri, A. M.; Cramer, C. J.; Farha, O. K., Presence Versus Proximity: The Role of Pendant Amines in the Catalytic Hydrolysis of a Nerve Agent Simulant. *Angew. Chem. Int. Ed.* **2018,** *57* (7), 1949-1953.
37. Horcajada, P.; Serre, C.; Vallet-Regí, M.; Sebban, M.; Taulelle, F.; Férey, G., Metal–Organic Frameworks as Efficient Materials for Drug Delivery. *Angew. Chem.* **2006,** *118* (36), 6120-6124.
38. Huxford, R. C.; Della Rocca, J.; Lin, W., Metal-Organic Frameworks as Potential Drug Carriers. *Curr. Opin. Chem. Biol.* **2010,** *14* (2), 262-268.
39. Bloch, E. D.; Queen, W. L.; Krishna, R.; Zadrozny, J. M.; Brown, C. M.; Long, J. R., Hydrocarbon Separations in a Metal-Organic Framework with Open Iron(Ii) Coordination Sites. *Science* **2012,** *335* (6076), 1606-1610.
40. DeCoste, J. B.; Peterson, G. W., Metal-Organic Frameworks for Air Purification of Toxic Chemicals. *Chem. Rev.* **2014,** *114* (11), 5695-727.
41. Bobbitt, N. S.; Mendonca, M. L.; Howarth, A. J.; Islamoglu, T.; Hupp, J. T.; Farha, O. K.; Snurr, R. Q., Metal-Organic Frameworks for the Removal of Toxic Industrial Chemicals and Chemical Warfare Agents. *Chem. Soc. Rev.* **2017,** *46* (11), 3357-3385.
42. Islamoglu, T.; Atilgan, A.; Moon, S.-Y.; Peterson, G. W.; DeCoste, J. B.; Hall, M.; Hupp, J. T.; Farha, O. K., Cerium(Iv) Vs Zirconium(Iv) Based Metal–Organic Frameworks for Detoxification of a Nerve Agent. *Chem. Mater.* **2017,** *29* (7), 2672-2675.
43. Howarth, A. J.; Katz, M. J.; Wang, T. C.; Platero-Prats, A. E.; Chapman, K. W.; Hupp, J. T.; Farha, O. K., High Efficiency Adsorption and Removal of Selenate and Selenite from Water Using Metal-Organic Frameworks. *J. Am. Chem. Soc.* **2015,** *137* (23), 7488-7494.
44. Khan, N. A.; Jung, B. K.; Hasan, Z.; Jhung, S. H., Adsorption and Removal of Phthalic Acid and Diethyl Phthalate from Water with Zeolitic Imidazolate and Metal-Organic Frameworks. *J. Hazard. Mater.* **2015,** *282*, 194-200.
45. Howarth, A. J.; Wang, T. C.; Al-Juaid, S. S.; Aziz, S. G.; Hupp, J. T.; Farha, O. K., Efficient Extraction of Sulfate from Water Using a Zr-Metal-Organic Framework. *Dalton Trans.* **2016,** *45* (1), 93-97.
46. Cavka, J. H.; Jakobsen, S.; Olsbye, U.; Guillou, N.; Lamberti, C.; Bordiga, S.; Lillerud, K. P., A New Zirconium Inorganic Building Brick Forming Metal Organic Frameworks with Exceptional Stability. *J. Am. Chem. Soc.* **2008,** *130* (42), 13850-13851.
47. Audu, C. O.; Nguyen, H. G. T.; Chang, C.-Y.; Katz, M. J.; Mao, L.; Farha, O. K.; Hupp, J. T.; Nguyen, S. T., The Dual Capture of Asvand Asiiiby Uio-66 and Analogues. *Chem. Sci.* **2016,** *7* (10), 6492-6498.
48. Drout, R. J.; Otake, K.; Howarth, A. J.; Islamoglu, T.; Zhu, L.; Xiao, C.; Wang, S.; Farha, O. K., Efficient Capture of Perrhenate and Pertechnetate by a Mesoporous Zr Metal–Organic Framework and Examination of Anion Binding Motifs. *Chem. Mater.* **2018,** *30* (4), 1277-1284.

49. Yabushita, M.; Li, P.; Durkin, K. A.; Kobayashi, H.; Fukuoka, A.; Farha, O. K.; Katz, A., Insights into Supramolecular Sites Responsible for Complete Separation of Biomass-Derived Phenolics and Glucose in Metal-Organic Framework Nu-1000. *Langmuir* **2017,** *33* (17), 4129-4137.
50. Katz, M. J.; Brown, Z. J.; Colon, Y. J.; Siu, P. W.; Scheidt, K. A.; Snurr, R. Q.; Hupp, J. T.; Farha, O. K., A Facile Synthesis of Uio-66, Uio-67 and Their Derivatives. *ChemComm* **2013,** *49* (82), 9449-9451.
51. Islamoglu, T.; Otake, K.-i.; Li, P.; Buru, C. T.; Peters, A. W.; Akpinar, I.; Garibay, S. J.; Farha, O. K., Revisiting the Structural Homogeneity of Nu-1000, a Zr-Based Metal–Organic Framework. *CrystEngComm* **2018,** *20* (39), 5913-5918.
52. Lyu, J.; Zhang, X.; Otake, K.-i.; Wang, X.; Li, P.; Li, Z.; Chen, Z.; Zhang, Y.; Wasson, M. C.; Yang, Y.; Bai, P.; Guo, X.; Islamoglu, T.; Farha, O. K., Topology and Porosity Control of Metal–Organic Frameworks through Linker Functionalization. *Chem. Sci.* **2019**, 10.1039/C8SC04220A.
53. Wang, T. C.; Vermeulen, N. A.; Kim, I. S.; Martinson, A. B.; Stoddart, J. F.; Hupp, J. T.; Farha, O. K., Scalable Synthesis and Post-Modification of a Mesoporous Metal-Organic Framework Called Nu-1000. *Nat. Protoc* **2016,** *11* (1), 149-162.
54. Chavan, S.; Vitillo, J. G.; Gianolio, D.; Zavorotynska, O.; Civalleri, B.; Jakobsen, S.; Nilsen, M. H.; Valenzano, L.; Lamberti, C.; Lillerud, K. P.; Bordiga, S., H2storage in Isostructural Uio-67 and Uio-66 Mofs. *PCCP* **2012,** *14* (5), 1614-1626.
55. Kica, M.; Ronka, S., The Removal of Atrazine from Water Using Specific Polymeric Adsorbent. *Sep. Sci. Technol.* **2014,** *49* (11), 1634-1642.
56. Yan, X. M.; Shi, B. Y.; Lu, J. J.; Feng, C. H.; Wang, D. S.; Tang, H. X., Adsorption and Desorption of Atrazine on Carbon Nanotubes. *J. Colloid Interface Sci.* **2008,** *321* (1), 30-38.
57. Zhao, X.; Ouyang, W.; Hao, F.; Lin, C.; Wang, F.; Han, S.; Geng, X., Properties Comparison of Biochars from Corn Straw with Different Pretreatment and Sorption Behaviour of Atrazine. *Bioresour. Technol.* **2013,** *147*, 338-344.
58. El-Sheikh, A. H.; Sweileh, J. A.; Al-Degs, Y. S.; Insisi, A. A.; Al-Rabady, N., Critical Evaluation and Comparison of Enrichment Efficiency of Multi-Walled Carbon Nanotubes, C18 Silica and Activated Carbon Towards Some Pesticides from Environmental Waters. *Talanta* **2008,** *74* (5), 1675-1680.
59. Zhou, Y.; Zhang, F.; Tang, L.; Zhang, J.; Zeng, G.; Luo, L.; Liu, Y.; Wang, P.; Peng, B.; Liu, X., Simultaneous Removal of Atrazine and Copper Using Polyacrylic Acid-Functionalized Magnetic Ordered Mesoporous Carbon from Water: Adsorption Mechanism. *Sci. Rep.* **2017,** *7*, 43831.
60. Chaparadza, A.; Hossenlopp, J. M., Adsorption Kinetics, Isotherms and Thermodynamics of Atrazine Removal Using a Banana Peel Based Sorbent. *Water Sci. Technol.* **2012,** *65* (5), 940-947.
61. Lladó, J.; Lao-Luque, C.; Ruiz, B.; Fuente, E.; Solé-Sardans, M.; Dorado, A. D., Role of Activated Carbon Properties in Atrazine and Paracetamol Adsorption Equilibrium and Kinetics. *Process Saf. Environ. Prot.* **2015,** *95*, 51-59.
62. Iarc Working Group on the Evaluation of Carcinogenic Risk to Humans. Some Chemicals That Cause Tumours of the Kidney or Urinary Bladder in Rodents and Some Other Substances. Lyon (Fr): International Agency for Research on Cancer; 1999. (Iarc Monographs on the Evaluation of Carcinogenic Risks to Humans, No. 73.) 1, Exposure Data. https://www.ncbi.nlm.nih.gov/books/NBK402084/ (accessed 16 June).